Optimization of laboratory illumination in optical dating

Sohbati, Reza; Murray, Andrew ; Lindvold, Lars René; Buylaert, Jan-Pieter; Jain, Mayank

Published in:
Quaternary Geochronology

Link to article, DOI:
10.1016/j.quageo.2017.02.010

Publication date:
2017

Document Version
Peer reviewed version

Accepted Manuscript

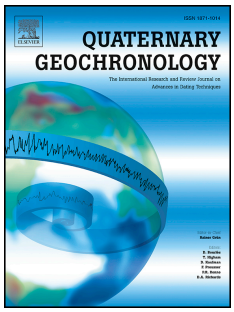

Optimization of laboratory illumination in optical dating

Reza Sohbati, Andrew Murray, Lars Lindvold, Jan-Pieter Buylaert, Mayank Jain

PII: S1871-1014(16)30160-1

DOI: 10.1016/j.quageo.2017.02.010

Reference: QUAGEO 831

To appear in: *Quaternary Geochronology*

Received Date: 31 October 2016

Revised Date: 10 February 2017

Accepted Date: 21 February 2017

Please cite this article as: Sohbati, R., Murray, A., Lindvold, L., Buylaert, J.-P., Jain, M., Optimization of laboratory illumination in optical dating, *Quaternary Geochronology* (2017), doi: 10.1016/j.quageo.2017.02.010.

Optimization of laboratory illumination in optical dating

Reza Sohbati[1,*], Andrew Murray[2], Lars Lindvold[1], Jan-Pieter Buylaert[1,2], Mayank Jain[1]

[1]Center for Nuclear Technologies, DTU Nutech, Technical University of Denmark, Roskilde

[2]Nordic Laboratory for Luminescence Dating, Department of Geoscience, Aarhus University

*corresponding author: resih@dtu.dk

Abstract

As part of the development of new laboratory lighting, we present a methodological approach applicable to the characterization of any light source intended for illumination in optical dating laboratories. We derive optical absorption cross-sections for quartz and feldspar from published data and compare these with the human eye response. The optimum peak wavelength giving the best clarity of non-dark adapted vision for the least trapped charge loss lies within the wavelength range 590 to 630 nm; we argue that it is unnecessary to consider dark-adapted vision. The predicted relative decay rates of quartz optically stimulated luminescence (OSL) and feldspar infrared stimulated luminescence (IRSL) signals by an incandescent light bulb and a compact fluorescent lamp (CFL) through an ILFORD 902 filter are first derived. These predicted decay rates are then compared with those of three relevant light-emitting diodes (LEDs); this comparison demonstrates the significant advantage of the LED sources over the filtered light sources, because essentially all of the reduction of both OSL and IRSL signals by the LEDs occurs at wavelengths to which the human eye is most sensitive. We conclude that exposure of quartz and feldspar extracts from various samples to the light from an LED with emission peak at 594 nm results in a $\leq$ 1% OSL or IRSL signal loss for a 48-hour exposure at a power density of ~0.2 $\mu W.cm^{-2}$.

Keywords: optical dating, laboratory illumination, optimization, LED

1. Introduction

A prerequisite for the reliable measurement of a light-sensitive trapped charge population is that the original population remains unaffected during any treatment prior to measurement (see section 3.2.2 in Aitken, 1998). Ambient lighting in optical dating laboratories is a significant source of concern, and should be kept as low as possible. On the other hand, laboratory pretreatment of samples before measurement often involves significant personal hazard (e.g. hydrofluoric acid) and working several hours per day under dim light condition; there is thus an obligation to demonstrate that the intensity of ambient lighting is not unnecessarily low.

Optimization of ambient lighting in luminescence dating laboratories has been subject to several studies since the early days of thermoluminescence (TL) dating. Almost all of these are published in Ancient TL. The first studies focused on blocking wavelengths < 550 nm by conversion of white fluorescent tubes to safelights using UV-green absorbing filters (Sutton and Zimmerman, 1978; Jensen and Barbetti, 1979; Spooner and Prescott, 1986; Spooner et al., 1988). Filtered white fluorescent tubes were chosen over red bulbs and red fluorescent tubes because they provided better clarity of vision (Sutton and Zimmerman, 1978). However, the batch-to-batch variation in the transmittance of color filters as pointed out by Smith (1988) and the general convenience of lighting without any additional filtering prompted further investigation into unfiltered colored light sources (Galloway and Napier, 1991; Galloway, 1991) even after the advent of optically stimulated luminescence (OSL) dating of quartz which makes use of traps that are more sensitive to light than those used in TL dating (Huntley et al., 1985).

With the introduction of infrared stimulated luminescence (IRSL) dating of feldspars (Hütt et al., 1988) and the recognition of an IR absorption resonance at ~850 nm as at least partially responsible for age underestimation (Aitken, 1994), later studies aimed at reducing the IR component of laboratory lights as well as blocking wavelengths < 550 nm. For instance, Lamothe (1995) used a combination of red filters with a bandpass glass filter to limit the emission spectrum of white fluorescent tubes to 600-650 nm, while Spooner et al. (2000) developed a light module consisted of a low-pressure sodium vapor lamp emitting predominantly at 589 nm screened with five layers of yellow plastic filters to reject the high energy photons; this light module was later adopted by others (e.g. Mauz et al., 2002). Spooner et al. (2000) rightly argued that yellow-orange wavelengths are not considerably more effective at luminescence signal reduction (bleaching) than orange-red wavelengths; since the operator's eye

is more sensitive to yellow-orange, these wavelengths can be used at a lower intensity. This argument was also used by Huntley and Baril (2002) who obtained their IR-suppressed yellow-orange laboratory light by placing orange filters in front of compact fluorescent light (CFL) bulbs (Huntley and Baril, 2002).

Given the narrow emission band and ready power control of light emitting diodes (LEDs) compared to incandescent light bulbs and CFLs, Berger and Kratt (2008) tested the suitability of a green and a red LED for laboratory illumination. They deduced that exposure of quartz to either of these LEDs at an intensity of ~0.7 $\mu W.cm^{-2}$ will have no significant effect on the OSL signal for up to few hours, while the safe exposure time for feldspar IRSL signal was found to be 30-40 min. and 15-20 min. for the green and red LED, respectively. Although such exposure times are rather short for most routine laboratory procedures, no guidance on a practical combination of light intensity and exposure time was provided (Berger and Kratt, 2008). Moreover, these green and red wavelengths are distant from the yellow-orange light discussed by previous workers (e.g. Spooner et al., 2000; Huntley and Baril, 2002). Consequently, despite their long-known unreliable characteristics (Smith, 1988), color filters have remained popular sources of laboratory safelights in optical dating; our own laboratory has, for example, consistently used ILFORD 902 glass filters (developed for photographic processing), but these are no longer available.

As existing laboratories undergo renovation and new laboratories are established, there is a constant demand for new laboratory light sources; this demand is also stimulated by laboratory intercomparisons and the dating of standard samples (Murray et al., 2015). Unfortunately, there are no standard methods for determining ambient light conditions, and as a consequence there is, in our view, a tendency to adopt the principle of ‘the darker and redder the better’. However, such an approach can lead to unsafe laboratory practices, and so the development of a methodological approach to the optimization of ambient illumination is of crucial importance.

The choice of the optimum light source for illumination in an optical dating laboratory hinges on the answers to two questions: first of all, what is the most appropriate wavelength for exposure, given the optical absorption cross-sections of quartz and feldspar, and the light response of the human eye? Secondly, given some minimum exposure time required for sample preparation in the laboratory, what is the maximum power density to which grains of quartz and feldspar can be exposed at this wavelength before any loss of the trapped charge of interest

becomes unacceptable? To address these questions, we first derive the quartz OSL and feldspar IRSL optical absorption cross-sections from published data and divide these into the known response of the human eye to determine the wavelength region providing the best clarity of vision for the least trapped charge loss – not surprisingly this lies within the yellow-orange region. The emission spectra of the widely-used ILFORD 902 safelights and three relevant commercially-available LEDs are measured to determine the relative effect of the peak emission compared to the short and long wavelength tails on the reduction of the quartz and feldspar signals. The most suitable light source is then tested extensively on samples of various geological origins (Table 1) to determine the maximum acceptable power density for a given exposure time.

2. Instrumentation and measurement conditions

Spectral measurements were carried out using an Ocean Optics MAYA2000-Pro spectrometer with a spectral range of 200-1100 nm. All spectra were measured over a total integration time of 150 s and corrected for detector non-linearity, electrical dark current and stray light. The power densities were measured with a Thorlabs PM200 handheld optical power meter console equipped with a Thorlabs S120VC photodiode power sensor with an aperture diameter of 9.5 mm. The luminescence measurements were performed on a Risø TL/OSL reader with an automated Detection And Stimulation Head (DASH, Model TL-DA 20) (Lapp et al., 2015). The blue light (470 nm, ~100 $mW.cm^{-2}$) stimulated signal from quartz grains was detected through a combination of a 2.5- and a 5-mm-thick Hoya U-340 glass filters (FWHM at the net transmittance peak at 340 nm = 90 nm) and the infrared (870 nm, ~175 $mW.cm^{-2}$) stimulated signal from K-rich feldspar and polymineral fine grains was measured through a blue filter pack composed of a 3-mm-thick Schott BG3 and a 2-mm-thick Schott BG39 filter (FWHM at the net transmittance peak at 400 nm = 130 nm). Beta irradiations used a $^{90}Sr/^{90}Y$ source mounted on the reader and calibrated for stainless steel disks using 180-250 µm calibration quartz grains (Hansen et al., 2015). Grains were mounted as medium (~4 mm diameter) or large (~8 mm diameter) aliquots in a monolayer using silicone oil on 9-mm-diameter stainless steel discs. All thermal treatments and stimulations at temperatures higher than 200 °C were carried out in nitrogen atmosphere, and a pause of 5 s was inserted before stimulation to allow all grains to reach the measurement temperature. The heating rate was 5 $°C.s^{-1}$ throughout. Data was collected for ~0.8

s before and after optical stimulation to monitor any isothermal thermoluminescence (ITL) signals.

OSL measurements were carried out for 40 s at 125^{o}C with a preheat temperature of 260^{o}C for 10 s and a cut-heat (thermal treatment after test dose) temperature of 220^{o}C. IR stimulations were performed at 50^{o}C for 100 s with a pre-thermal treatment at 250^{o}C for 60 s. OSL signal intensities were calculated using the initial 0.32 s of the signal minus an immediate background derived from the following 0.8 s. The IRSL signal was derived from the first second of stimulation less a background from the last 10 s.

3. Methodology

Finding an ideal laboratory light source that provides reasonable illumination but no depletion of trapped charge populations is challenging. Quartz OSL and feldspar IRSL signals are derived from trapped charges that can be excited by photons over a wide range of wavelengths, from the visible to the near infrared (e.g. Hütt et al., 1988; Bailiff and Poolton, 1991; Ditlefsen and Huntley, 1994; Bøtter-Jensen et al., 1994; Spooner 1994a, b). Furthermore, although the human eye is sensitive over nine orders of magnitude, its wavelength-dependent sensitivity changes as a function of the absolute intensity: at low illumination levels the peak sensitivity of the human eye shifts toward the blue end of the color spectrum (the Purkinje shift); while the cone-dominated photopic vision under well-lit conditions (> 0.001 cd.m^{-2}, e.g. fairly bright moon) has peak response at 555 nm, the response of the rod-dominated scotopic vision under low-light conditions (< 0.001 cd.m^{-2}, e.g. moonless clear night sky) peaks at 507 nm (Pokorny, 1979).

Figure 1 presents the photopic and scotopic human eye responses together with the optical absorption cross-sections as a function of wavelength for both quartz OSL and feldspar IRSL signals, based on the bleaching response data from Spooner (1994a,b). At wavelengths >500 nm, feldspar IRSL bleaches more rapidly than quartz OSL, whereas at shorter wavelengths quartz OSL is much more sensitive to light. The two human eye responses peak in the wavelength region where the two cross-sections are comparable.

To determine the wavelengths at which the best compromise between clarity of vision and bleaching is achieved, in Figure 2 we divide the human eye response by the optical absorption cross-section to give what we define as the ‘desirability’ function. The maxima of this function

identify, for the two human eye responses, the wavelengths that ensure minimum bleaching of quartz OSL and feldspar IRSL signals for best clarity of vision. Figure 2 shows that for a human eye in photopic mode these maxima occur at 631 nm and 592 nm for quartz and feldspar, respectively, while the corresponding maxima for scotopic vision are found at wavelengths ~50 nm shorter. The changeover from photopic to scotopic vision at ~0.001 $cd.m^{-2}$ corresponds to an intensity of ~0.5 $nW.cm^{-2}$ at 555 nm, orders of magnitude lower than the typical light levels of ~0.1 $\mu W.cm^{-2}$ regarded as 'safe' in the literature (e.g. Huntley and Baril, 2002). This indicates that the shift to scotopic vision does not happen in optical dating laboratories under routine conditions and is thus irrelevant to our study. We therefore only consider the photopic 'desirability' peaks in further analysis.

4. Results

We now investigate the relative bleaching rates of different light sources on quartz OSL and feldspar IRSL signals. This is carried out by multiplying the measured emission spectra of each light source by the photoionization cross-sections of the two signals (see Fig. 1) to derive their relative bleaching rates over a wide wavelength range (300 to 1100 nm). The resulting bleaching spectra are then compared with the desired peaks identified above (see Fig. 2) to evaluate the importance to bleaching of the wavelengths to which the human eye is insensitive. Finally, the actual bleaching effect on quartz OSL and feldspar IRSL signals of the most suitable light source is characterized using various samples.

4.1. ILFORD 902

Many optical dating laboratories around the world use ILFORD safelight filters to remove and/or attenuate the harmful wavelengths to quartz OSL and feldspar IRSL signals of incandescent light bulbs or CFLs. Figure 3 presents the measured emission spectra of a 25-W Osram incandescent light bulb and an 11-W Cosna CFL through an ILFORD 902 filter. The emission of the incandescent light bulb has a significant infrared component > 700 nm that is not completely stopped by the ILFORD 902 filter, while the filtered spectrum of the CFL is dominated by strong mercury (Hg) lines within the desired zone. The products of these spectra with the quartz OSL and feldspar IRSL optical cross-sections (Fig.1) are shown in Figures 4 and 5. From Figure 4 it can be seen that most of the bleaching of OSL and IRSL signals by the

filtered emission of the incandescent light bulb occurs at wavelengths that are not visible to human eye, making it a very inefficient light source for laboratory illumination. On the other hand, the relative bleaching rate under the CFL is dominated by the region of optimum human eye response. This is clearly a significant improvement over the incandescent light bulb, but unfortunately there is still a significant component that can potentially cause the bleaching of quartz OSL at wavelengths < 400 nm.

4.2. Light-emitting diodes

Light emitting diodes (LEDs) provide much more efficient (~20×) and durable (~100×) light sources than incandescent light bulbs (Schubert and Kim, 2005; Bright, 2014), and have a much narrower emission band (typical Full Width at Half Maximum, FWHM ~20 nm) (Talbott and Clifford, 2012). Such characteristics suggest that LEDs should be very attractive alternative light sources for illumination in optical dating laboratories.

Figure 6 shows the measured emission spectra of three LEDs with peak emissions at 626 nm, 621 nm and 594 nm, close to the desirable wavelengths identified in Fig. 2. However, these diodes also appear to have emission tails both at long and short wavelengths (see inset to Fig. 6). In order to test whether these tails are real or a measurement artefact, we measured the emission spectrum of the 594 nm diode through a series of long-pass filters with cut-off wavelengths ranging from 280 nm to 550 nm. If the tails are real, one would expect them to be significantly attenuated by these filters. However, Figure 7 shows there is, in fact, no significant systematic attenuation of the apparent emission spectrum, indicating that the 'tails' are a measurement artefact, presumably caused by stray light inside the spectrometer.

As before, we evaluate the importance to bleaching of the wavelengths to which the human eye is insensitive by considering the product of the spectra from Figure 6 and the cross sections from Figure 1. Figure 8 shows that essentially all of the bleaching of both OSL and IRSL signals occurs at wavelengths to which the human eye is most sensitive. This is a significant improvement compared to ILFORD 902 lamps, especially because no filtering of the LEDs' spectra is required. It is also concluded that the apparent bleaching of OSL by wavelengths outside the desirable range is a measurement artefact, as discussed above.

Of the three LEDs tested above, that with peak emission at 594 nm is the most efficient for our purposes, because the relative perception of brightness by the eye at this wavelength (orange)

is ~76%, twice the perception at 621 nm (red; ~38% - see Fig. 1). Thus the 594 nm LED would provide the same visibility as the 621 nm LED, but at half the power density. Since the bleaching rates at the two wavelengths are almost equal, and 594 nm is further from the feldspar IR resonance at 850 nm than the 621 nm emission, the 594 nm diode was selected for further testing.

5. Bleaching tests

Having identified the most appropriate wavelength and light source, the next step is to determine the bleaching response of quartz OSL and feldspar IRSL signals to this wavelength. This will allow the quantification of any of the three parameters of signal loss, power density and exposure time, by setting the desired values of the other two. To this end, 48 aliquots each of Risø calibration quartz (Hansen et al., 2015) and K-rich feldspar from a loess sample (sample D38139) were prepared. Seven sets of 6 aliquots were bleached by the 594 nm LED with a power density of ~12.7 $\mu W.cm^{-2}$ at the sample position for various lengths of time from 45 min. to 72 h. The eighth set was kept in the dark (unexposed) as a reference. The intact and residual quartz OSL and K-feldspar IR_{50} signals (L_n) and their response to test dose (T_n) were then measured for all the aliquots. Figure 9 shows the ratio of the average L_n/T_n from each exposed group to the corresponding average from the unexposed set, as a function of light exposure time. We fit the OSL data by a single-exponential decay function assuming that the initial signal is dominated by the fast component (Jain et al., 2005), while the fit to IR_{50} data is obtained using the model of Jain et al. (2015) (Fig. 9). Using the best-fit values for model parameters and assuming a < 1% loss of signal after 48 h of exposure is acceptable, the upper limit to the power densities for quartz and feldspar are calculated to be 0.35 $\mu W.cm^{-2}$ and 0.22 $\mu W.cm^{-2}$, respectively.

In order to confirm that the values of power density estimated above are indeed safe for use with samples of different grain size and geological origin, we measured the bleaching effect of the 594 nm LED on coarse- and fine-grained quartz and feldspar fractions extracted from samples of various geological origins. Details of sample location and preparation can be found in the respective references (Table 1). Of the 12 aliquots prepared from each sample, six were exposed to the LED with power density of ~12.7 $\mu W.cm^{-2}$ at the aliquots' position for 24 h, and the other six were kept unexposed as reference. The quartz OSL and feldspar IR_{50} L_n/T_n ratios

were then measured for all the aliquots (Fig. 9). The variation in the experimentally observed ratios suggests an apparent difference in signal loss from sample to sample (Fig. 9). The reduction in OSL varies from 9±9% (sample 072255) to 30±10% (sample 981009), and the reduction in IR_{50} ranges from 27±8% (sample 075403) to 50±8% (sample A4, polymineral fine-grain) (Fig. 9). If the observed variation in bleaching rate is real, an upper limit to safe light intensity must be defined based on the sample that bleaches most rapidly. The bleaching rate of the OSL signal from different quartz samples was calculated assuming a single-exponential decay and the decay rate of the IR_{50} signal was derived by simultaneous fitting of the data using Jain et al.'s (2015) model, assuming the same ratio of excitation and relaxation probabilities and the same attempt-to-tunnel frequency for all the samples. The power density required for 1% signal reduction after 48 h of exposure was then calculated based on the best-fit values of model parameters. The predicted power densities range from 0.18 to 0.67 $\mu W.cm^{-2}$ for quartz OSL and from 0.23 to 0.32 $\mu W.cm^{-2}$ for feldspar IRSL (Table 1).

6. Discussion

The overall higher bleaching rate of feldspar IRSL than quartz OSL at 594 nm makes feldspar the determining factor for setting the upper limit to power density and the exposure duration in the laboratory; this applies to almost all the samples studied here, with the exception of sample 981009, for which the two signals seem to be reduced by the same amount (~ 30%) after 24 h of exposure. The higher than expected apparent bleaching rate of this OSL signal may arise from feldspar contamination within the quartz grains in this sample, previously identified by Murray and Funder (2003).

In general, there seems to be a significant variation in both quartz and feldspar signal loss from sample to sample. This may indicate a genuine difference in the bleaching response of quartz OSL and feldspar IRSL signals in samples of different origin, possibly arising from variations in optical transmission of grains due to size, color and transparency (Duller, 1997; Jain et al., 2003).

It is also important to note that the actual emission peak of an LED may be different than the nominal peak reported by the manufacturer; this was the case for one of the LEDs used in this study (nominal 614 nm, actual 594 nm). In addition, not all LEDs have a narrow emission band with a single peak. For example, we tested a nominally green LED with a broad major peak at

543 nm and a minor peak at 427 nm (Fig. S1). Clearly any LED with potential application to laboratory lighting should be characterized and tested before use.

7. Conclusion

A methodological approach to the characterization of light sources suitable for illumination in optical dating laboratories has been presented. Based on published data, we argued that the best compromise between minimum bleaching and maximum visibility is achieved at a wavelength range from ~590 to 630 nm. Comparison of the predicted relative bleaching rates of quartz OSL and feldspar IRSL signals by an incandescent light bulb and a CFL through an ILFORD 902 filter with those of three different LEDs with peak emission in the wavelength range mentioned above shows that the LEDs have a great advantage over the ILFORD filtered light sources, because essentially all of the bleaching of both OSL and IRSL signals by the LEDs occurs at wavelengths to which the human eye is most sensitive. The efficiency of the eye at 590 nm is > 3 times than that at 630 nm, and so the LEDs with peak emission close to 590 nm are preferred as they can provide the same visibility at ~1/3 intensity.

We conclude that the bleaching response of quartz OSL and feldspar IRSL signals from various samples to an LED with emission peak at 594 nm results in a ≤ 1% signal loss for a 48-hour exposure at a power density of ~0.2 $\mu W.cm^{-2}$. This is an improvement by a factor of ~5 compared to the sodium lamp of Spooner et al. (2000), which gave a calculated IRSL bleaching rate of 1.2%/day at 0.1 $\mu W.cm^{-2}$ and is ~3 times better than Huntley and Baril's (2002) filtered fluorescent lamp, which gave an IRSL reduction of 0.07%/h at 0.2 $\mu W.cm^{-2}$. The power density of 0.2 $\mu W.cm^{-2}$ is well above the dark-adaption threshold of the human eye and in our opinion provides a comfortable laboratory illumination level. This value is also probably conservative as it is obtained by direct exposure in air of clean grains (after chemical treatment) to the light source. In reality, such direct exposure only takes place for a short time during the mounting of grains on the substrate (i.e. disks or cups) immediately before the measurement. For much of the earlier sample preparation, including sieving, acid treatment and heavy liquid separation, grains are either in turbid suspensions, covered by surface coatings, or suspended in liquid in beakers.

LEDs are easily-accessible, cheap, efficient and durable light sources of readily adjustable power whose nearly monochromatic emission band eliminates the need for any additional filtering. Given the rapid transition of lighting industries to LEDs, incandescent light bulbs and

CFLs are likely to be more difficult to obtain in the future. All these factors indicate that LEDs are an attractive, reliable alternative to the conventional light sources currently used for illumination in optical dating laboratories.

Acknowledgments

Louise Maria Helsted, Lars Peter Pirtzel and Myungho Kook are gratefully acknowledged for their assistance with sample preparation and technical support with the electronics. J.-P.B. receives funding from the European Research Council (ERC) under the European Union's Horizon 2020 research and innovation programme ERC-2014-StG 639904 – RELOS.

References

Aitken, M.J., 1994. Optical dating: a non-specialist review. *Quaternary Science Reviews*, *13*(5-7), pp.503-508.

Aitken, M. J., 1998. An Introduction to Optical Dating. 267 pp. Oxford University Press, Oxford.

Bailiff, I.K. and Poolton, N.R.J., 1991. Studies of charge transfer mechanisms in feldspars. *International Journal of Radiation Applications and Instrumentation. Part D. Nuclear Tracks and Radiation Measurements*, *18*(1), pp.111-118.

Bright, T., 2014. Efficient blue light-emitting diodes leading to bright and energy-saving white light sources. Scientific Background on the Noble Prize in Physics. https://www.nobelprize.org/nobel_prizes/physics/laureates/2014/advanced-physicsprize2014_2.pdf

Buylaert, J.P., Jain, M., Murray, A.S., Thomsen, K.J., Thiel, C. and Sohbati, R., 2012. A robust feldspar luminescence dating method for Middle and Late Pleistocene sediments. *Boreas*, *41*(3), pp.435-451.

Buylaert, J.P., Yeo, E.Y., Thiel, C., Yi, S.W., Stevens, T., Thompson, W., Frechen, M., Murray, A. and Lu, H.Y., 2015. A detailed post-IR IRSL chronology for the last interglacial soil at the Jingbian loess site (northern China). *Quaternary Geochronology*, *30*, pp.194-199.

Bøtter-Jensen, L., Duller, G.A.T. and Poolton, N.R.J., 1994. Excitation and emission spectrometry of stimulated luminescence from quartz and feldspars. *Radiation Measurements*, *23*(2-3), pp.613-616.

Ditlefsen, C. and Huntley, D.J., 1994. Optical excitation of trapped charges in quartz, potassium feldspars and mixed silicates: the dependence on photon energy. *Radiation Measurements*, *23*(4), pp.675-682.

Duller, G.A.T., 1997. Behavioural studies of stimulated luminescence from feldspars. *Radiation Measurements*, *27*(5), pp.663-694.

Galloway, R.B. and Napier, H.J., 1991. Alternative laboratory illumination: ‘gold’fluorescent tubes. *Ancient TL*, *9*, pp.6-9.

Galloway, R.B., 1991. The bleaching of latent optically stimulated luminescence. *Ancient TL*, *9(3)*, pp.47-49

Hansen, V., Murray, A.S., Buylaert, J.-P., Yeo, E.Y. and Thomsen, K.J., 2015. A new irradiated quartz for beta source calibration. *Radiation Measurements*, *81*, pp.123-127.

Huntley, D.J., Godfrey-Smith, D.I. and Thewalt, M.L., 1985. Optical dating of sediments. *Nature*

Huntley, D.J. and Baril, M.R., 2002. Yet another note on laboratory lighting. *Ancient TL*, *20*, pp.39-40.

Hütt, G., Jaek, I. and Tchonka, J., 1988. Optical dating: K-feldspars optical response stimulation spectra. *Quaternary Science Reviews*, *7*(3), pp.381-385.

Jain, M., Murray, A.S. and Bøtter-Jensen, L., 2003. Characterisation of blue-light stimulated luminescence components in different quartz samples: implications for dose measurement. *Radiation Measurements*, *37*(4), pp.441-449.

Jain, M., Murray, A.S., Bøtter-Jensen, L. and Wintle, A.G., 2005. A single-aliquot regenerative-dose method based on IR bleaching of the fast OSL component in quartz. *Radiation Measurements*, *39*(3), pp.309-318.

Jain, M., Sohbati, R., Guralnik, B., Murray, A.S., Kook, M., Lapp, T., Prasad, A.K., Thomsen, K.J. and Buylaert, J.P., 2015. Kinetics of infrared stimulated luminescence from feldspars. *Radiation Measurements*, *81*, pp.242-250.

Jensen, H. and Barbetti, M., 1979. More on filters for laboratory illumination. *Ancient TL*, *7*(10).

Lamothe, M., 1995. Using 600–650 nm light for IRSL sample preparation. *Ancient TL*, *13*, pp.1-4.

Lapp, T., Kook, M., Murray, A.S., Thomsen, K.J., Buylaert, J.P. and Jain, M., 2015. A new luminescence detection and stimulation head for the Risø TL/OSL reader. *Radiation Measurements*, *81*, pp.178-184.

Mauz, B., Bode, T., Mainz, E., Blanchard, H., Hilger, W., Dikau, R. and Zöller, L., 2002. The luminescence dating laboratory at the University of Bonn: equipment and procedures. *Ancient TL*, *20*(2), pp.53-61.

Murray, A.S. and Funder, S., 2003. Optically stimulated luminescence dating of a Danish Eemian coastal marine deposit: a test of accuracy. *Quaternary Science Reviews*, *22*(10), pp.1177-1183.

Murray, A., Buylaert, J.P. and Thiel, C., 2015. A luminescence dating intercomparison based on a Danish beach-ridge sand. *Radiation Measurements*, *81*, pp.32-38.

Pokorny, Joel, ed. Congenital and Acquired Color Vision Defects. Grune & Stratton, 1979.

Schubert, E.F. and Kim, J.K., 2005. Solid-state light sources getting smart. *Science*, *308*(5726), pp.1274-1278.

Sharpe, L.T., Stockman, A., Jagla, W. and Jägle, H., 2005. A luminous efficiency function, V*(λ), for daylight adaptation. *Journal of Vision*, *5*(11), pp.3-3.

Smith, B.W., 1988. More cautions on laboratory illumination. *Ancient TL*, *6*(9), pp. 9.

Sohbati, R., Murray, A., Jain, M., Thomsen, K., Hong, S.C., Yi, K. and Choi, J.H., 2013. Na-rich feldspar as a luminescence dosimeter in infrared stimulated luminescence (IRSL) dating. *Radiation Measurements*, *51*, pp.67-82.

Spooner, N.A. and Prescott, J.R., 1986. A caution on laboratory illumination. *Ancient TL*, *4*(3), pp.46-48.

Spooner, N.A., Prescott, J.R. and Hutton, J.T., 1988. The effect of illumination wavelength on the bleaching of the thermoluminescence (TL) of quartz. *Quaternary Science Reviews*, *7*(3), pp.325-329.

Spooner, N.A., 1994a. On the optical dating signal from quartz. *Radiation Measurements*, *23*(2-3), pp.593-600.

Spooner, N.A., 1994b. The anomalous fading of infrared-stimulated luminescence from feldspars. *Radiation Measurements*, *23*(2), pp.625-632.

Spooner, N.A., Questiaux, D.G. and Aitken, M.J., 2000. The use of sodium lamps for low-intensity laboratory safelighting for optical dating. *Ancient TL*, *18*(2), pp.45-49.

Sun, J., Kohfeld, K.E. and Harrison, S.P., 2000. Records of aeolian dust deposition on the Chinese Loess Plateau during the Late Quaternary. Technical Reports—Max-Planck-Institut für Biogeochemie 1, 318.

Sutton, S.R. and Zimmerman, D.W., 1978. A blue-UV absorbing filter for laboratory illumination. *Ancient TL*, *5*(5).

Talbott C. M. and Clifford R. H., 2012. Characterization of light emitting diodes (LEDs) and compact fluorescent lamps (CFLs) by UV-Vis spectrophotometry, Shimadzu Scientific, http://www.ssi.shimadzu.com/products/literature/uv/VIS/SSI-Pittcon12-UV-001.pdf

Figure captions

Figure 1) The right axis shows the relative photopic (green, solid) and scotopic (blue, dashed) sensitivity of the human eye (Sharpe et al., 2005). The left axis shows the quartz (black, solid) and feldspar (red, dashed) optical absorption cross-sections calculated from the bleaching response spectra of Spooner (1994 a,b). The inset shows the same data on a linear scale.

Figure 2) The photopic- (solid) and scotopic- (dashed) sensitivity of the human eye divided by quartz and feldspar optical absorption cross-sections (data normalized).

Figure 3) The normalized emission spectra of an incandescent light bulb and a CFL, each through an ILFORD 902 filter. The black and red dashed lines show the quartz and feldspar 'desirability' curves, respectively, for photopic vision from Fig. 2.

Figure 4) The quartz OSL and feldspar IRSL relative bleaching rates due to an incandescent light bulb spectrum through an ILFORD 902 filter. The black and red dashed lines show the quartz and feldspar desirability curves, respectively, for photopic vision from Fig. 2.

Figure 5) The quartz OSL and feldspar IRSL relative bleaching rates due to a CFL spectrum through an ILFORD 902 filter. The black and red dashed lines show the quartz and feldspar desirability curves, respectively, for photopic vision from Fig. 2.

Figure 6) The spectra of three LEDs with peak emission within the desirability zone (logarithmic scale inset). The black and red dashed lines show the quartz and feldspar desirability curves, respectively, for photopic vision from Fig. 2. (The y-axis for the latter curves is not shown.)

Figure 7) The normalized emission spectra of the LED with peak emission at 594 nm through different long-pass filters (left y-axis) with the transmission shown on the right y-axis.

Figure 8) The quartz OSL and feldspar IRSL relative bleaching rates due to the selected LEDs. The black and red dashed lines show quartz and feldspar desirability curves, respectively, for photopic vision from Fig. 2.

Figure 9) The quartz OSL and feldspar IRSL bleaching response at 594 nm. The 24-hour data

point was measured for various samples. The open symbols show the recycling points. Each data point is an average of six aliquots. The error bars represent standard errors (n = 6).

Table captions

Table 1) Summary of the mineralogy, grain size, and calculated power density that results in 1% signal loss after 48 h of exposure for the samples used in this study.

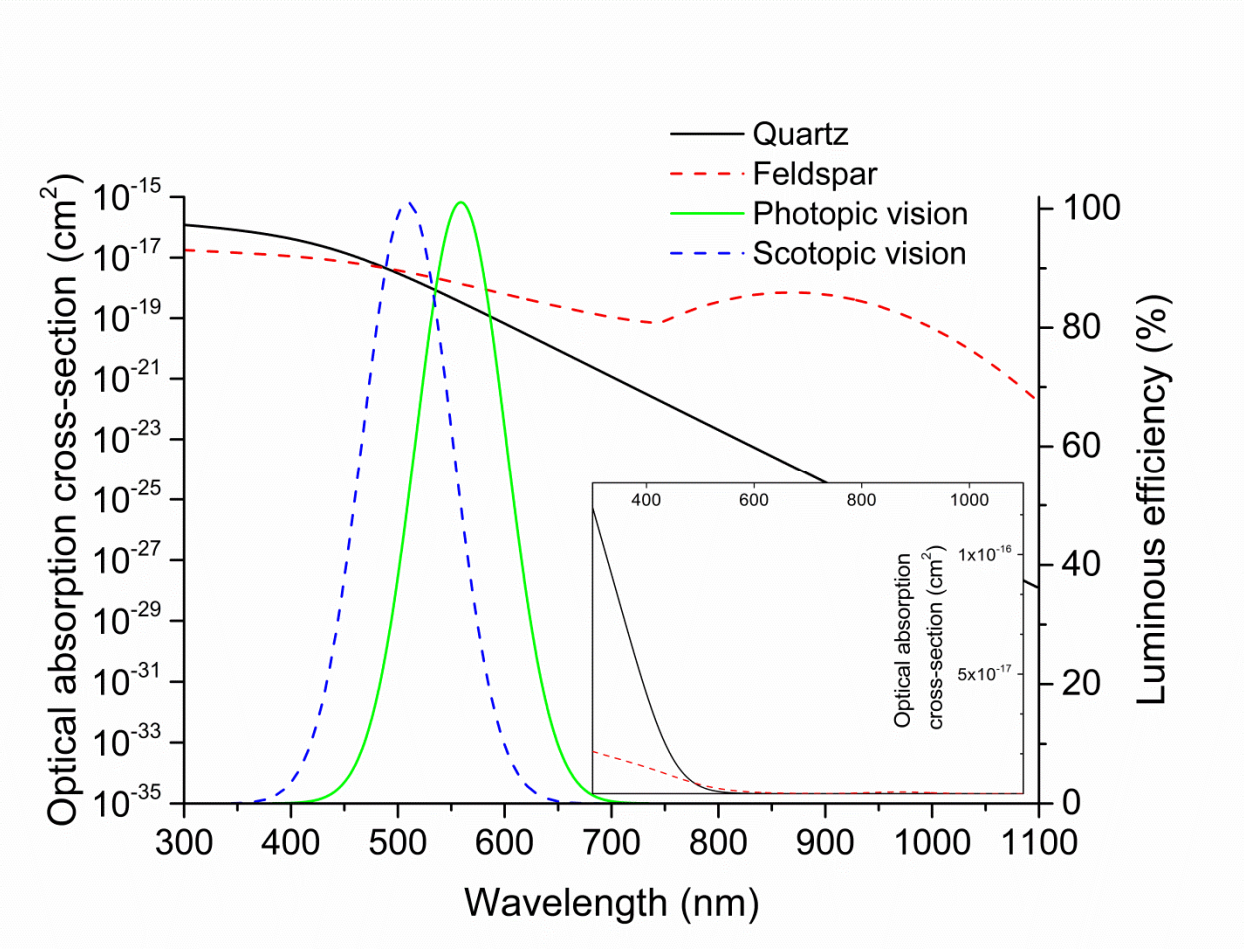

Figure 1

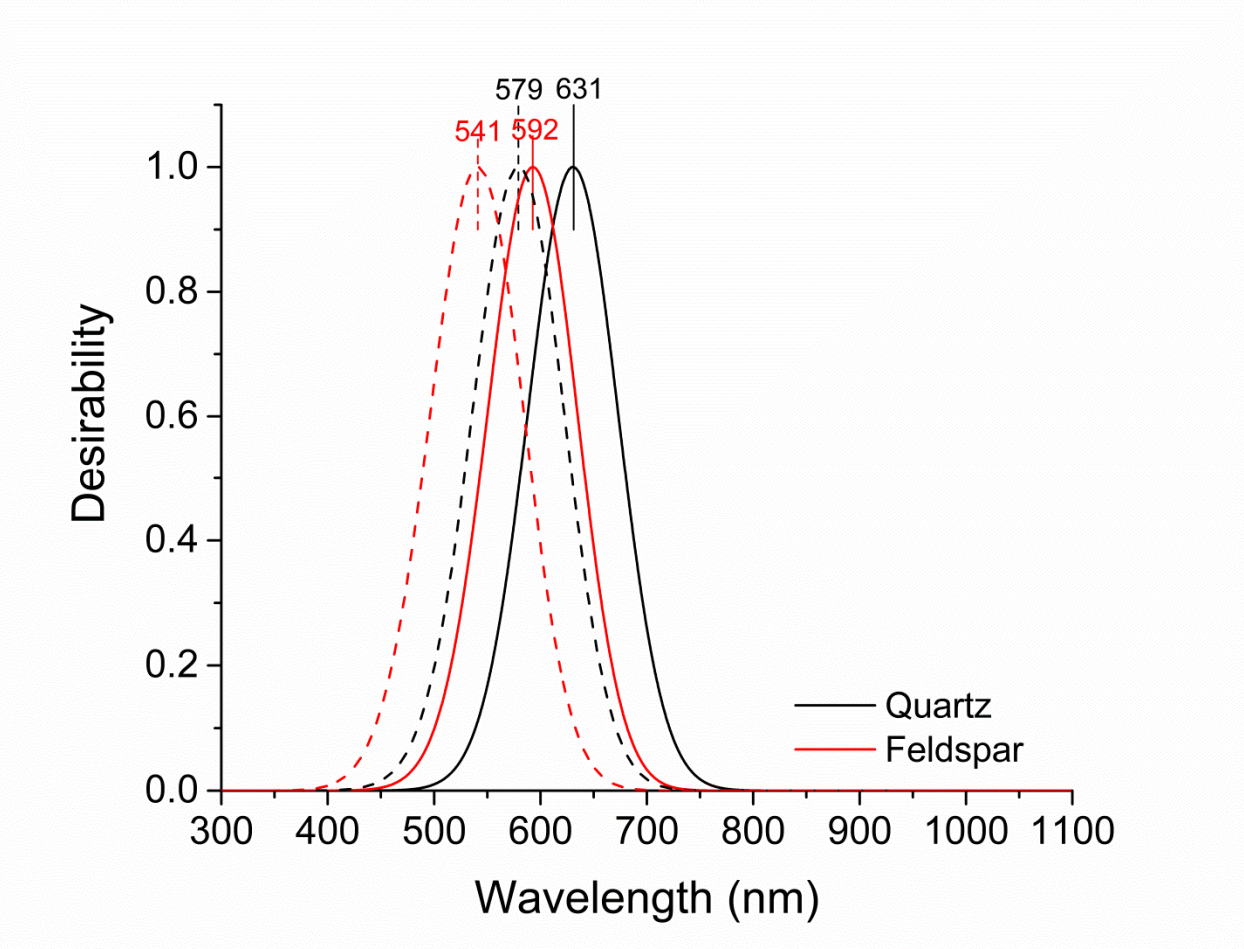

Figure 2

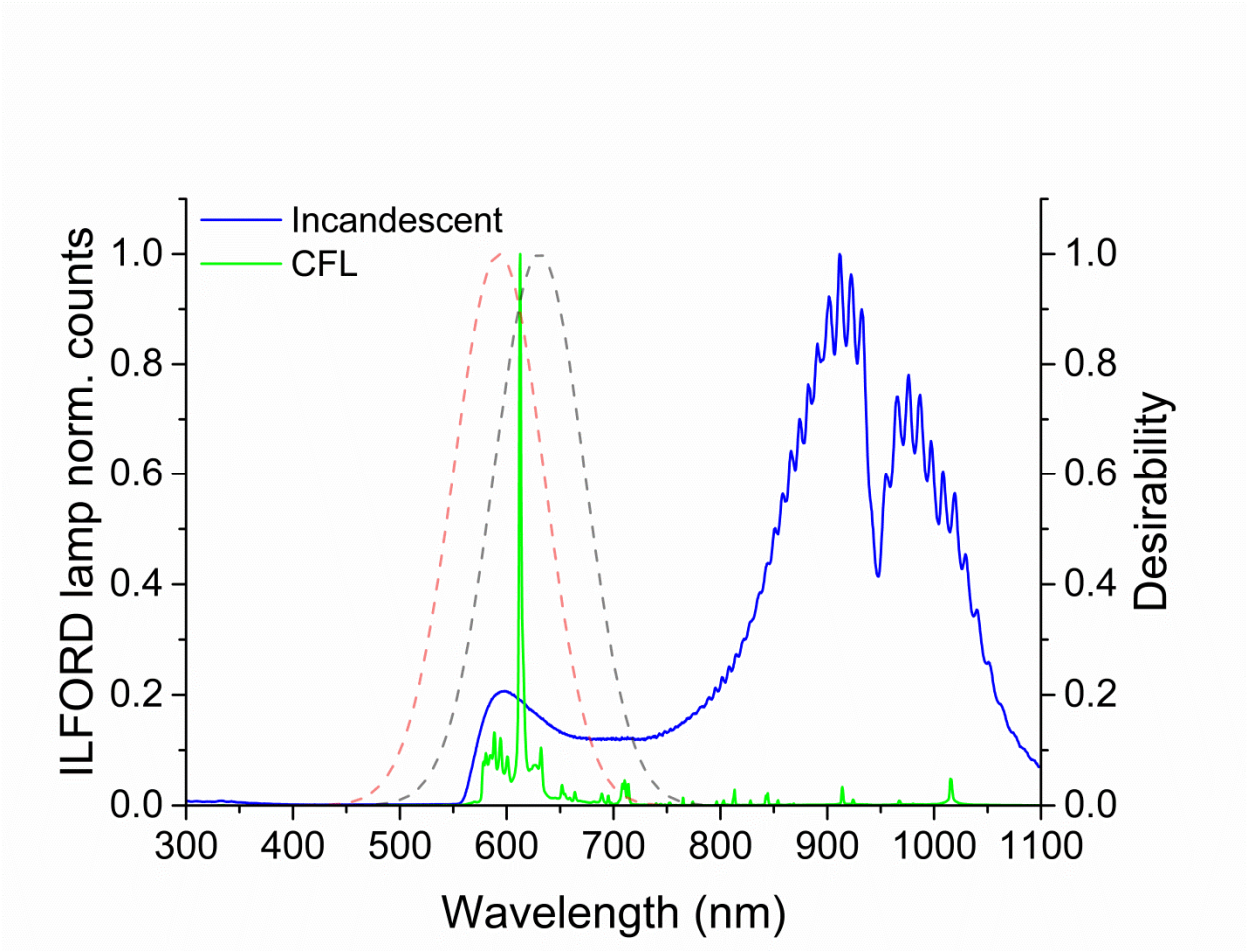

Figure 3

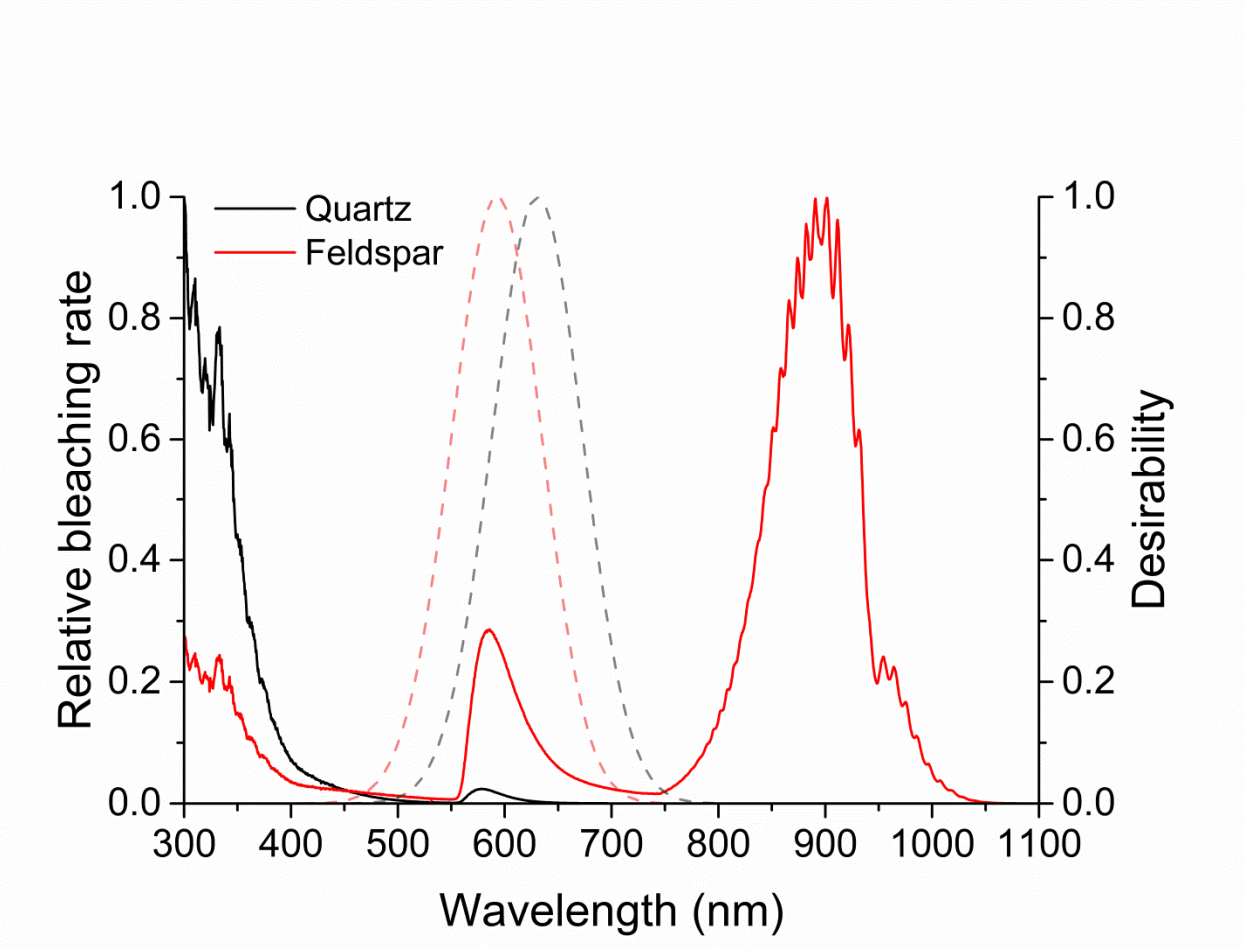

Figure 4

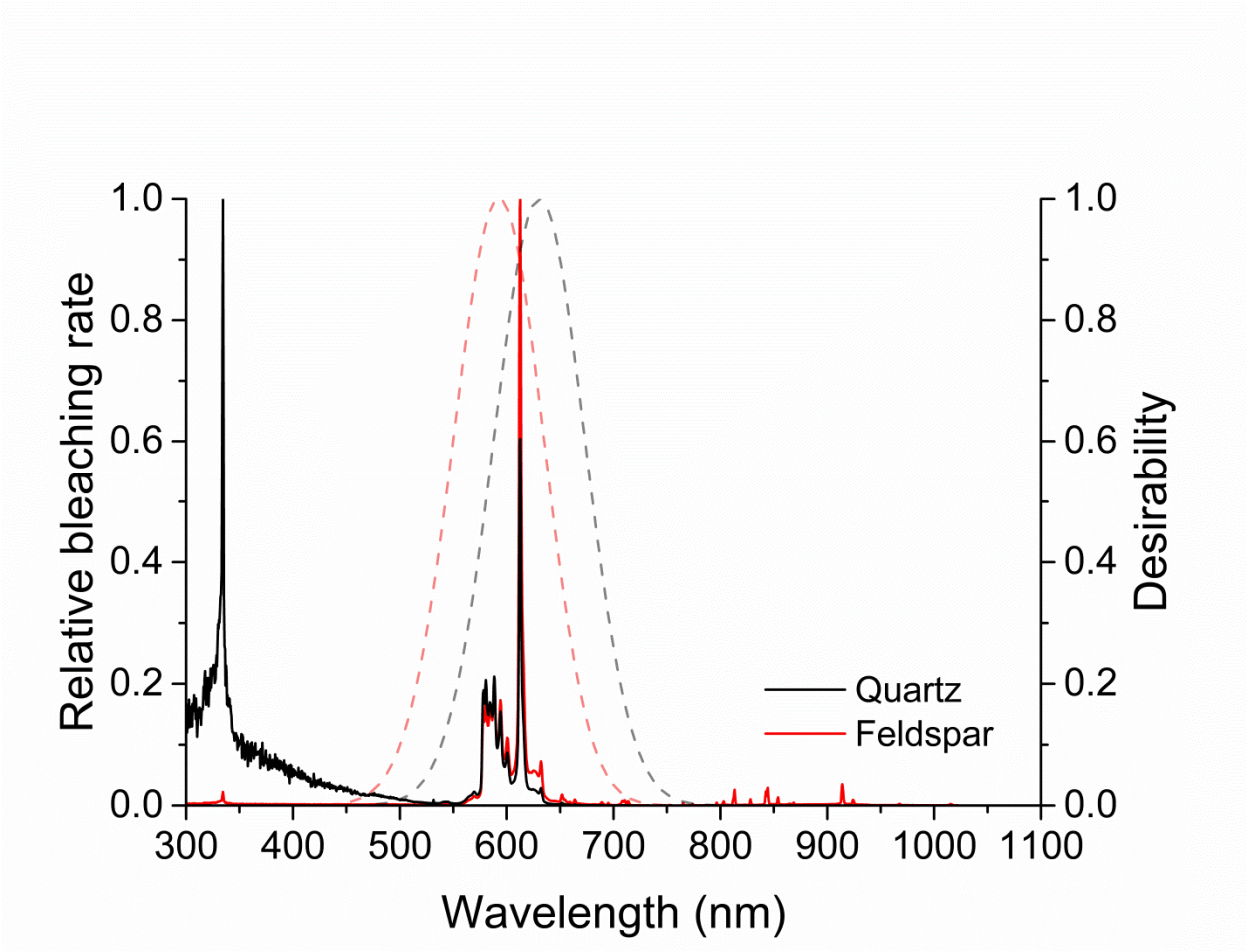

Figure 5

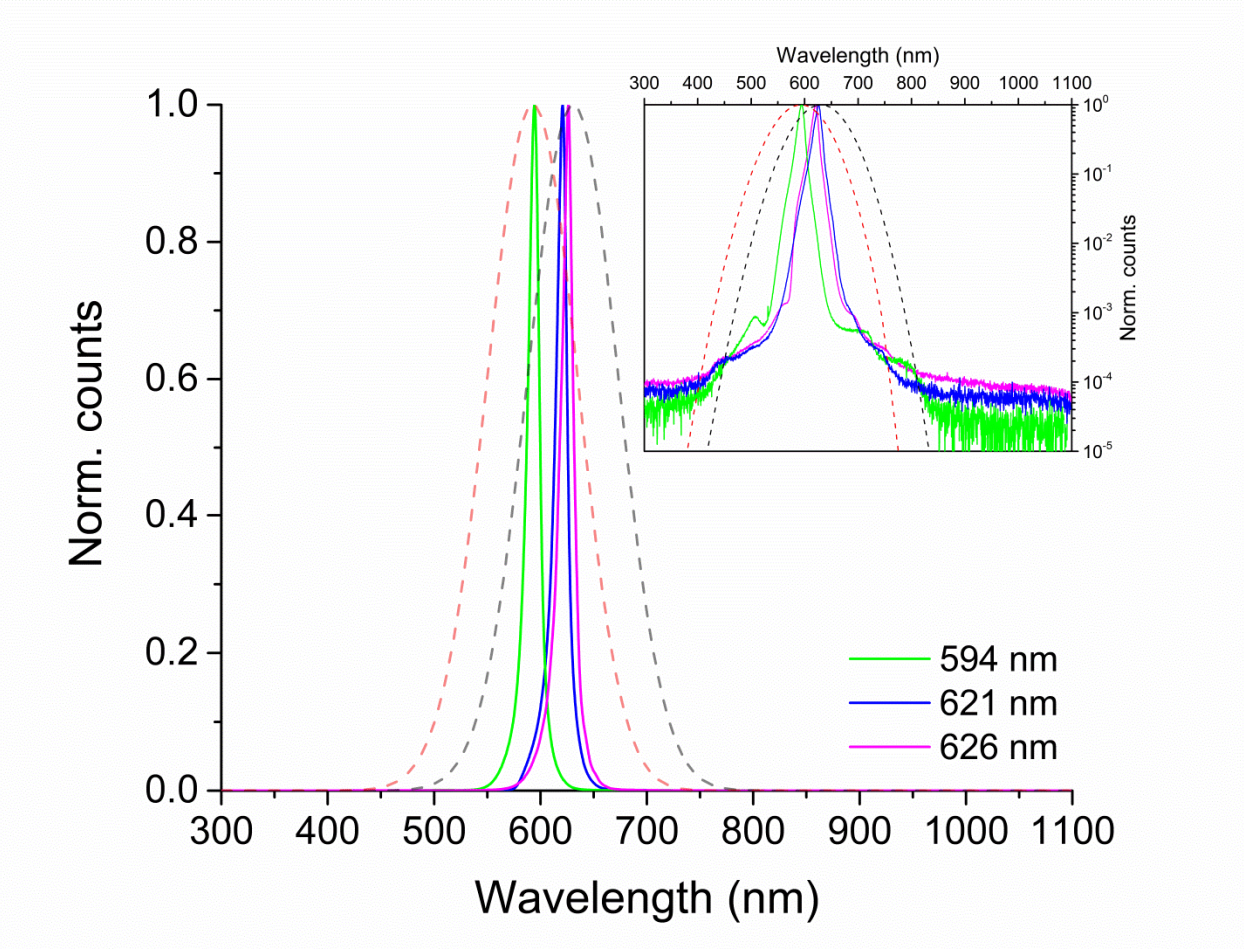

Figure 6

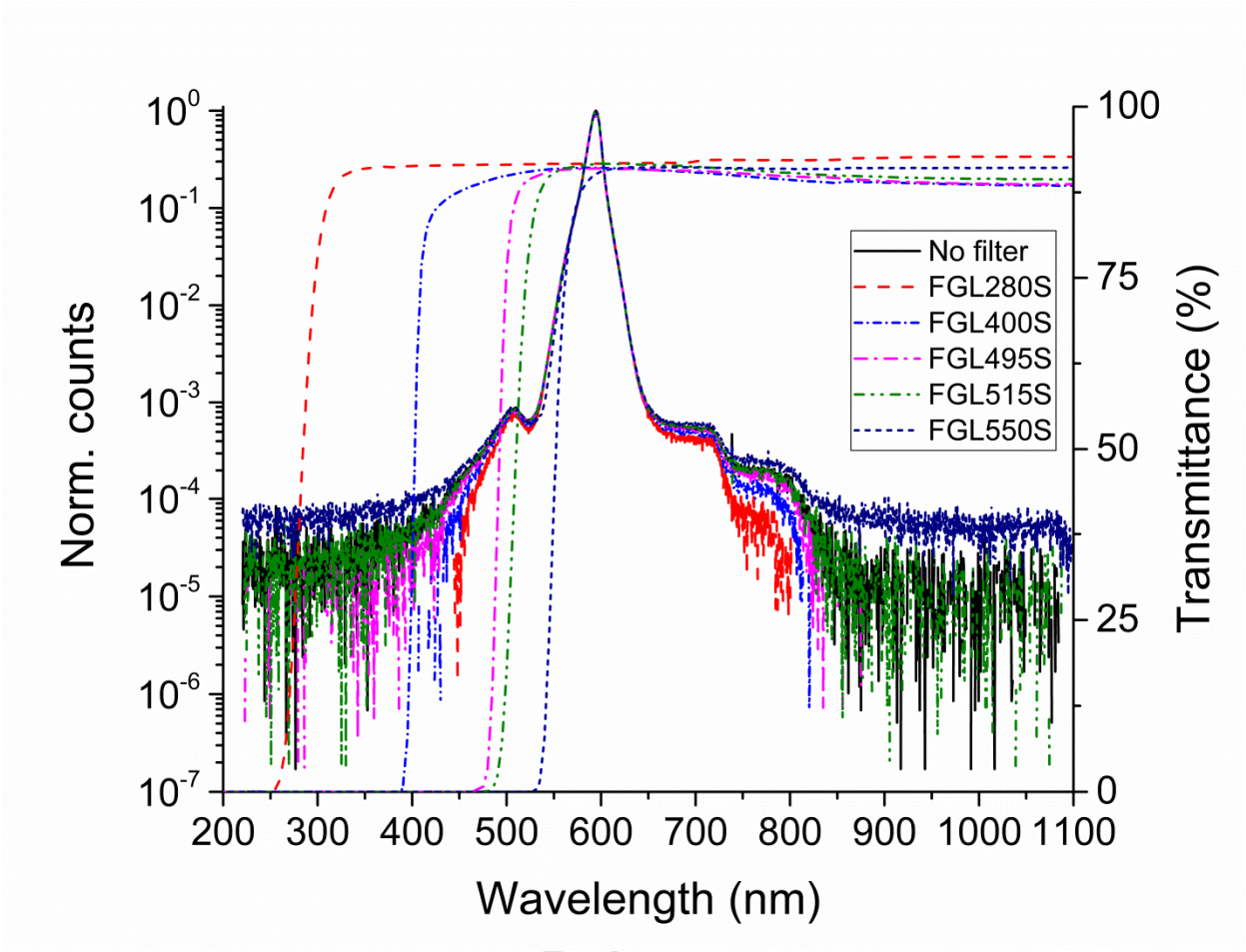

Figure 7

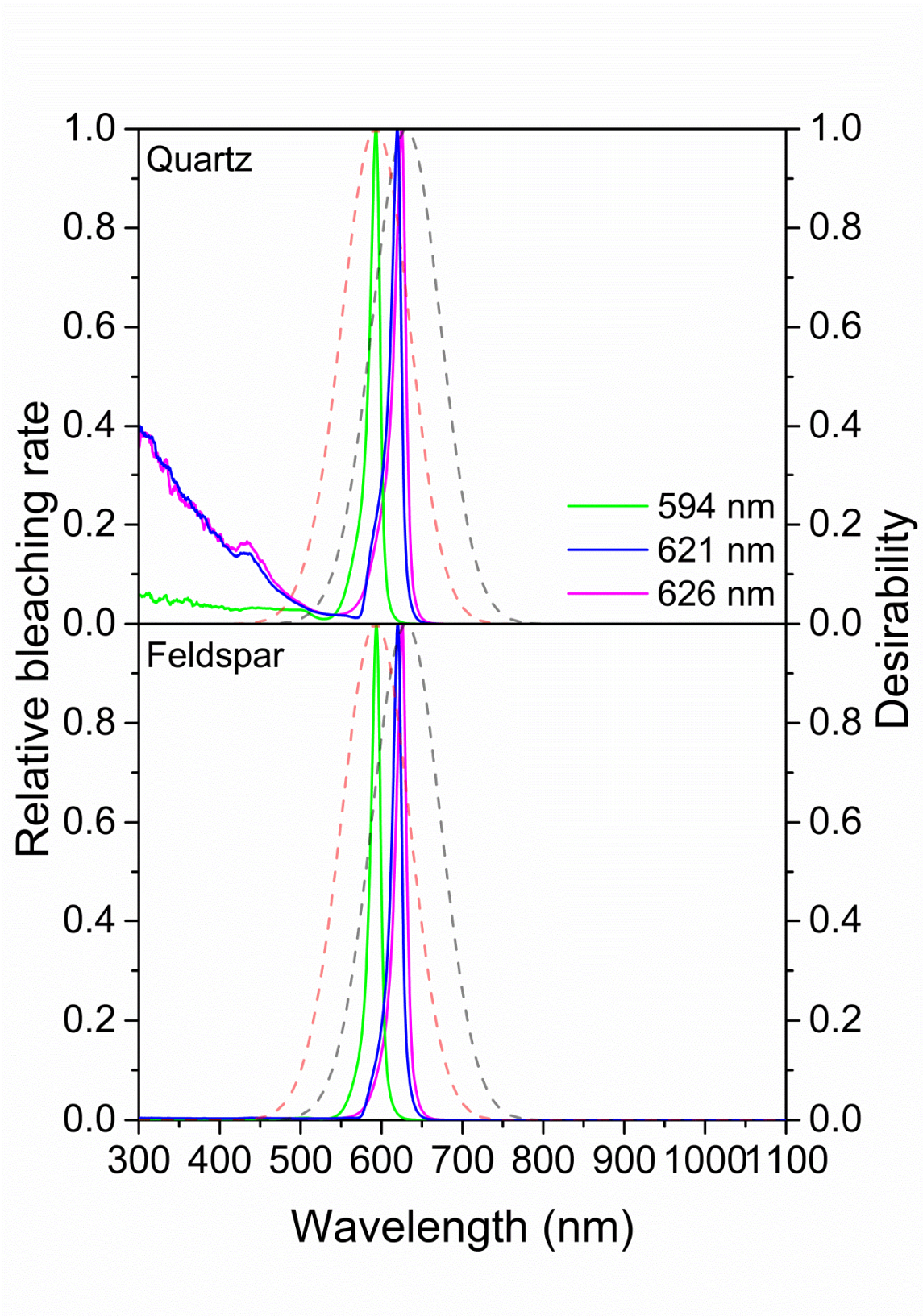
Quartz
Feldspar
594 nm
621 nm
626 nm
Relative bleaching rate
Desirability
Wavelength (nm)
1.0
0.8
0.6
0.4
0.2
0.0
300 400 500 600 700 800 900 1000 1100

Figure 8

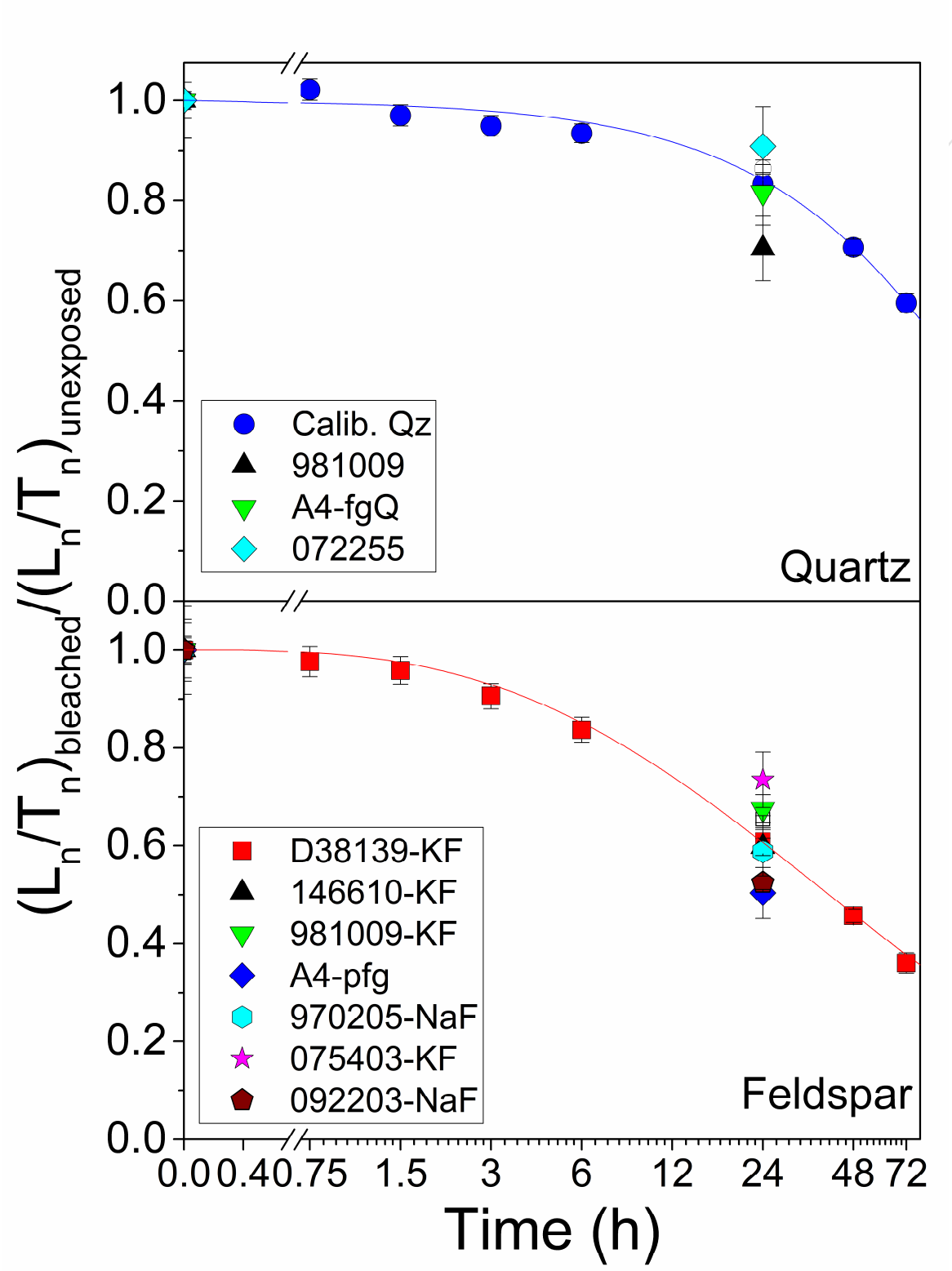
1.0
0.8
0.6
0.4
0.2
0.0
Calib. Qz
981009
A4-fgQ
072255
Quartz
D38139-KF
146610-KF
981009-KF
A4-pfg
970205-NaF
075403-KF
092203-NaF
Feldspar
0.0 0.4 0.75 1.5 3 6 12 24 48 72
Time (h)
(L_n/T_n)_bleached/(L_n/T_n)_unexposed

Figure 9

Table 1

Sample code	Sample type	Grain size µm	Calc. power density (µW.cm^{-2}) for 1%/48 h signal loss	Reference
Risø calib.	Quartz	180-250	0.37	Hansen et al. (2015)
981009	Quartz	150-250	0.18	Murray and Funder (2003)
A4	Quartz	4-11	0.31	This work*
072255	Quartz	180-250	0.67	Buylaert et al. (2012)
D38139	K-rich feldspar	90-180	0.26	This work*
146610	K-rich feldspar	40-63	0.25	Sohbati et al. (2016)
981009	K-rich feldspar	150-250	0.28	Buylaert et al. (2011)
075403	K-rich feldspar	180-250	0.32	Buylaert et al. (2012)
A4	polymineral	4-11	0.23	This work*
970205	Na-rich feldspar	90-300	0.25	Sohbati et al. (2013)
092203	Na-rich feldspar	90-180	0.23	Sohbati et al. (2013)

*A4 and D38139 are Chinese loess samples collected from last glacial loess (L1 unit). A4 was taken from a section at Duanjiapo (Sun et al., 2000) and D38139 from a section at Jingbian (~200 m from the S1 section from Buylaert et al., 2015).

Supplementary material

The emission spectrum of a nominally green LED with two broad emission peaks at 427 nm and 543 nm.

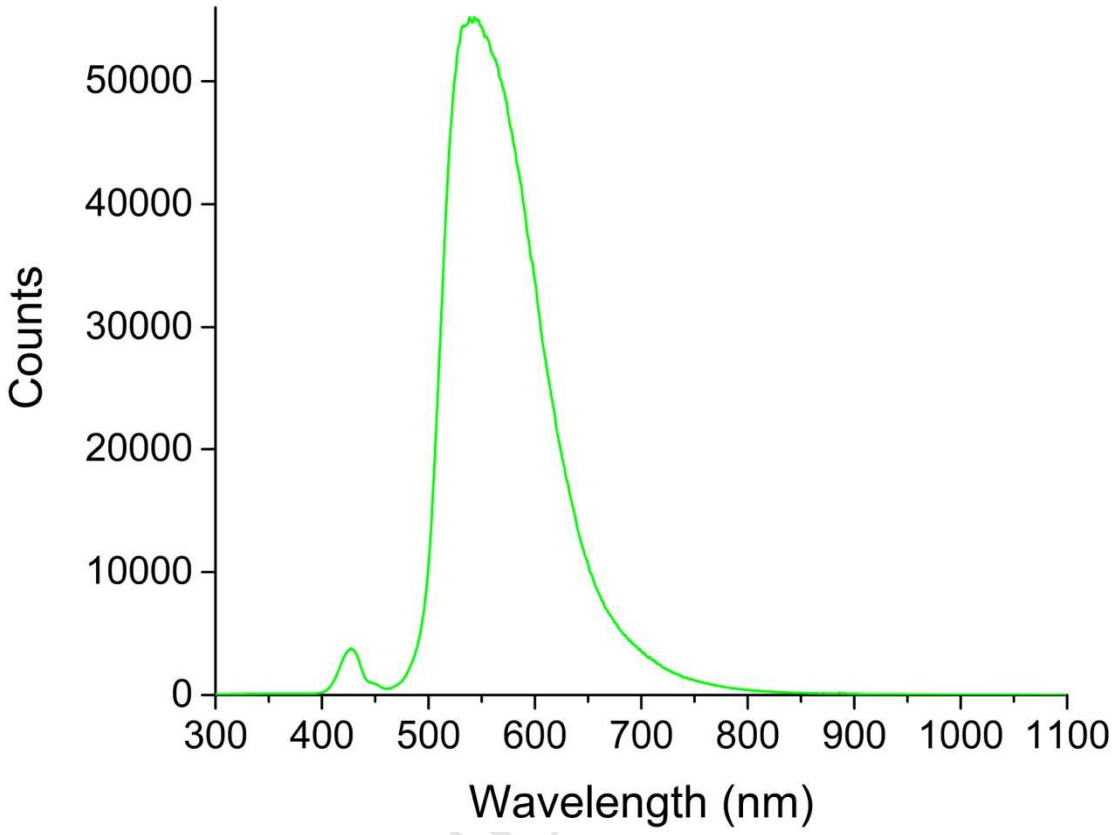

Figure S1)